Timing of Cenozoic volcanism and Basin and Range extension in northwestern Nevada: New constraints from the northern Pine Forest Range

Joseph P. Colgan[†]
Trevor A. Dumitru
Michael McWilliams
Elizabeth L. Miller
Department of Geological and Environmental Sciences, Stanford University, Stanford, California 94305-2115, USA

ABSTRACT

Eocene–middle Miocene volcanic rocks in the northern Pine Forest Range, Nevada, are ideally situated for reconstructing the timing and style of volcanism and extensional faulting in the northwesternmost part of the Basin and Range province. A conformable sequence of Cenozoic volcanic and sedimentary strata in the northern Pine Forest Range dips ~30°W, and 11 new $^{40}Ar/^{39}Ar$ ages from this sequence define 3 major episodes of volcanic activity. Pre-Tertiary basement and older (ca. 38 Ma) Tertiary intrusive rocks are overlain unconformably by Oligocene (ca. 30–23 Ma) basalt flows and dacitic to rhyolitic ash-flow tuffs interbedded with fine-grained tuffaceous sedimentary rocks. Oligocene rocks are overlain by ~550 m of ca. 17–16 Ma basalt flows equivalent to the Steens Basalt in southern Oregon, and basalt flows are capped by a thin 16.3 Ma ignimbrite that likely is correlative with either the Idaho Canyon Tuff or the Tuff of Oregon Canyon. The northern Pine Forest Range is bounded to the east by a major down-to-the-east normal fault that dips ~40°E with well-developed fault striations indicative of dip-slip motion. This fault initiated at an angle of ~70° and was rotated ~30° during uplift of the range. A suite of 17 apatite fission-track ages from the Pine Forest footwall block demonstrates that exhumation, uplift, and slip on the range-bounding fault began ca. 12–11 Ma and continued until at least 7 Ma, with moderate slip since then. The Pine Forest Range did not undergo significant extension before or during peak Oligocene and Miocene volcanism, and similar geologic relationships in nearby ranges suggest that a larger region of northwestern Nevada was also little extended during this interval. Basin and Range faulting in northwestern Nevada appears to have begun no earlier than 12 Ma, making it distinctly younger than deformation in much of central and southern Nevada, where peak extension occurred in the middle Miocene or earlier.

Keywords: Basin and Range, Pine Forest Range, volcanism, geochronology, fission-track dating.

INTRODUCTION

Modern ranges in the central part of the northern Basin and Range province (along lat 39°–40°N; Fig. 1) formed largely during a widespread episode of major normal fault slip ca. 19–14 Ma (Miller et al., 1999; Stockli, 1999; Stockli et al., 2001; Surpless et al., 2002). In many areas, these ranges cut and uplifted older extensional terranes that formed in the Eocene to early Miocene (e.g., Smith, 1992; Miller et al., 1999; Hudson et al., 2000; Egger et al., 2003; Howard, 2003), and the magnitude of Cenozoic extension totals 50%–100% (Smith et al., 1991). More recent (<12 Ma) Basin and Range extensional faulting has been concentrated largely at the eastern and western margins of the province and has generally involved more limited amounts of extension (e.g., Gilbert and Reynolds, 1973; Dilles and Gans, 1995; Armstrong et al., 2003; Stockli et al., 2003).

Basin and Range faulting is less well understood along the northern margin of the province in northwestern Nevada (Fig. 2). Extensional faulting in this region appears to be distinctly younger and of smaller magnitude than the widespread middle Miocene extension in the center of the province (Colgan et al., 2004). High fault-bounded ranges in this region give way northward to the high lava plateaus of southern Oregon, and the pre-Miocene tectonic history is obscured in many places by gently dipping Cenozoic lavas. Previous workers suggested that older Oligocene–early Miocene rocks in northwestern Nevada (Fig. 2) may record early Miocene(?) extensional faulting (Noble et al., 1970; Graichen, 1972), but the relevant units have not been studied in sufficient detail to properly characterize such faulting.

This study aims to better document the timing of Basin and Range extensional faulting and Cenozoic volcanism in northwestern Nevada and, in particular, to determine if there is evidence for extensional faulting prior to the late Miocene high-angle faulting that formed the modern ranges in the region. Well-preserved geologic relationships in the Pine Forest Range (Figs. 2, 3) are ideally suited for addressing these questions. Tertiary strata range from Oligocene to middle Miocene and are well exposed in a west-tilted, normal-fault-bounded crustal block (Noble et al., 1970; this study).

In this paper, we present new geologic mapping and $^{40}Ar/^{39}Ar$ ages of these Tertiary units, documenting a conformable 30–16 Ma volcanic and sedimentary sequence that shows no evidence for syndepositional faulting or tilting. The basement rocks exposed beneath the Tertiary sequence include abundant Jurassic-Cretaceous granitic plutons (Fig. 3) that permit the use of apatite fission-track thermochronology for dating the fault slip, tilting, and uplift that formed the range (e.g., Fitzgerald et al., 1991; Miller et al., 1999; Stockli et al., 2003). Fission-track data presented here document a single episode of major normal faulting that was ongoing from 12 to 7 Ma and continued into more recent times.

[†]Present address: U.S. Geological Survey, 345 Middlefield Road, MS 901, Menlo Park, California 94025, USA; e-mail: jcolgan@pangea.stanford.edu.

GSA Bulletin; January/February 2006; v. 118; no. 1/2; p. 126–139; doi: 10.1130/B25681.1; 8 figures; 2 tables; Data Repository item 2006013.

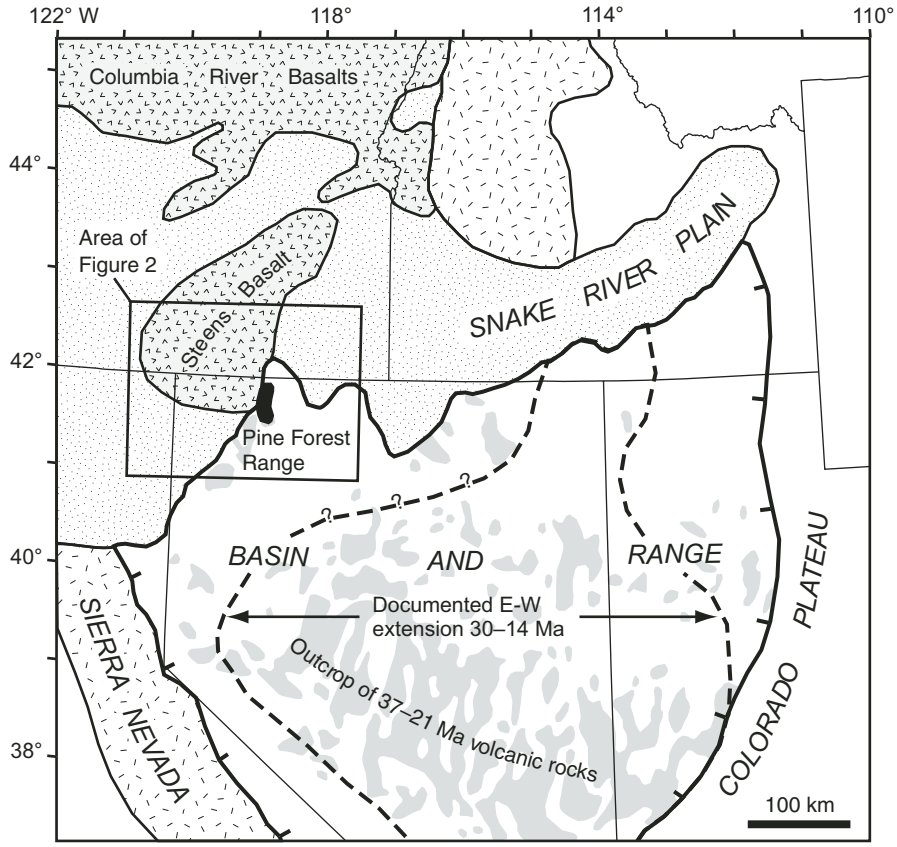

Figure 1. Map of part of western United States, showing major Cenozoic tectonic provinces (Wernicke, 1992), extent of Steens and Columbia River Basalts (Hooper et al., 2002), outcrop area of 37–21 Ma volcanic rocks (dark gray shading, from Christiansen and Yeats, 1992), and approximate extent of 30–15 Ma Basin and Range extension (Dilles and Gans, 1995).

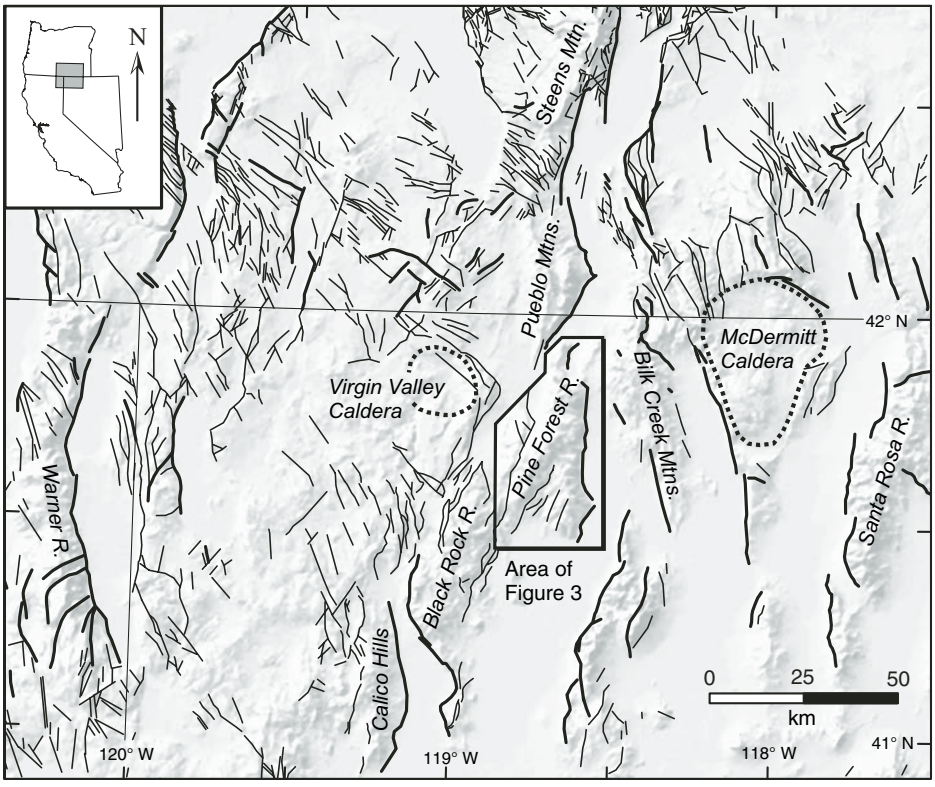

Figure 2. Shaded-relief map of northwestern Basin and Range province, showing features described in text. Faults from state geologic maps of Jennings et al. (1977), Stewart and Carlson (1978), and Walker and MacLeod (1991). McDermitt Caldera from Rytuba and McKee (1984); Virgin Valley Caldera from Castor and Henry (2000).

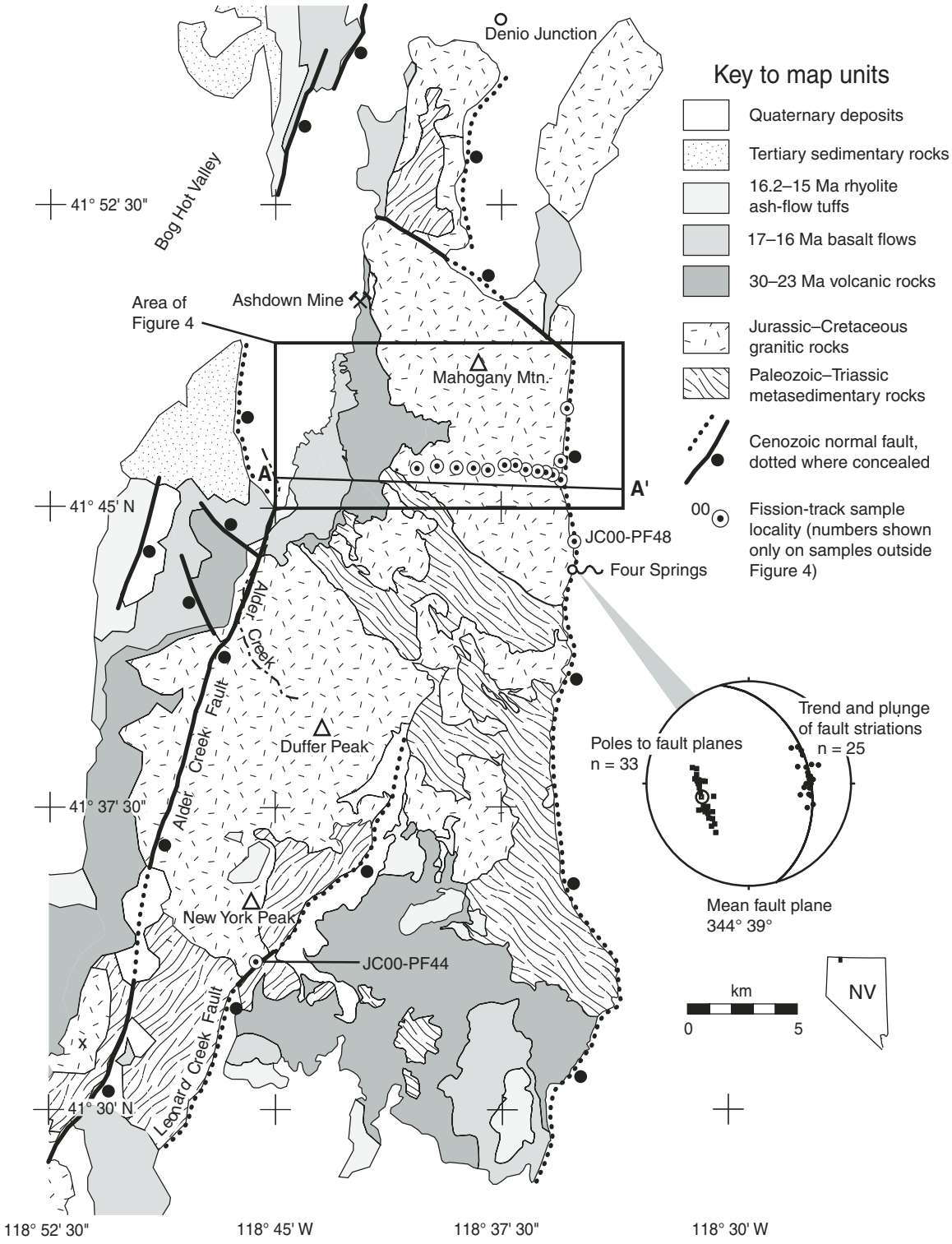

Figure 3. Generalized geologic map of Pine Forest Range, compiled from Smith (1973), Stewart and Carlson (1978), and Wyld (1996), with modifications and new mapping by the authors (this study, Fig. 4)

Together with regional data from nearby ranges, these new data indicate that Basin and Range extension in northwestern Nevada did not begin until the late Miocene, involved only a single generation of range-bounding normal faults, and accommodated moderate total amounts of extension (15%–20%).

PRE-TERTIARY GEOLOGY OF THE PINE FOREST RANGE

Basement rocks in the Pine Forest Range consist of Paleozoic to latest Triassic strata intruded by Jurassic and Cretaceous granitic plutons. Paleozoic strata include sedimentary and volcanic rocks that represent a Paleozoic arc system accreted to the continental margin during the Permo-Triassic Sonoma orogeny (Wyld, 1996). Overlying Mesozoic strata consist primarily of volcanogenic rocks related to development of the early Mesozoic continental margin arc (Wyld, 1996, 2002). Both Paleozoic and Mesozoic strata were deformed under greenschist- to amphibolite-facies conditions during southeast-northwest–directed shortening in Early to Middle Jurassic time, coeval with intrusion of Jurassic (200–185 Ma) plutons (Wyld, 1996). These metamorphic rocks are exposed as an intact, south-dipping crustal block in the southeastern part of the range (Fig. 3) that exposes progressively higher-grade, more deformed rocks from south to north. The tilting of this sequence postdates major Jurassic metamorphism and is thought to predate the intrusion of the Cretaceous (115–108 Ma) granitic plutons that now underlie much of the study area (Fig. 3; Wyld, 1996; Wyld and Wright, 2001). Wyld and Wright (2001) suggest that a major Early Cretaceous NNE-SSW–trending dextral strike-slip fault zone runs through the northern Pine Forest Range and may have accommodated tilting of the basement rocks and later localized intrusion of younger Cretaceous plutons.

TERTIARY IGNEOUS ROCKS OF THE PINE FOREST RANGE

Noble et al. (1970) described and named several volcanic units in the Pine Forest Range and nearby ranges, and Tertiary rocks in the southeastern part of the range were mapped and described by Smith (1973). Tertiary volcanic rocks in the study area (Figs. 3, 4) were previously mapped by Bryant (1970) and Graichen (1972). Miocene ash-flow tuffs from the McDermitt Caldera complex to the east (Fig. 3) were described and dated by Rytuba and McKee (1984) and Conrad (1984), and Miocene rhyolite lavas and ash flows from the Virgin Valley Caldera to the west (Fig. 3) were described and dated by Castor and Henry (2000).

Here, we present descriptions of the Tertiary volcanic rocks in the northern Pine Forest Range, together with new $^{40}Ar/^{39}Ar$ ages and geochemical data that establish the age and composition of the rocks in the study area. Field relationships are shown on the geologic map and cross section (Fig. 4), stratigraphic relationships are summarized in Figure 5, and geochronologic data are presented in Table 1 (also in Data Repository item, Part 1).[1] The geochemical data are shown in Figures 6 and 7 (also Table DR3; see footnote 1). Wherever possible, we recalculated cited $^{40}Ar/^{39}Ar$ ages to the same assumed monitor age used in this study (sanidine from the Taylor Creek Rhyolite; Duffield and Dalrymple, 1990), using the calibration factors of Renne et al. (1998). Recalculated ages are followed by "(TCs)" when quoted in the text; a listing of original and recalculated ages is available in Table DR4 (see footnote 1).

Trachyandesitic Intrusive Rocks

The oldest Tertiary rocks in the Pine Forest Range are commonly reddish-weathering, dark gray-green, porphyritic trachyandesites that contain abundant plagioclase and hornblende and lesser biotite phenocrysts in a fine-grained holocrystalline groundmass (unit Ta, Fig. 4). These rocks are poorly exposed and were previously mapped as lava flows (Graichen, 1972), but we interpret them as hypabyssal intrusive rocks on the basis of their outcrop patterns (mapped largely from float) and coarsely porphyritic textures. Biotite from one small intrusion yielded a $^{40}Ar/^{39}Ar$ plateau age of 38.21 ± 0.29 Ma (Fig. 5).

Older Basalt Flows

South and west of Fisher Peak (Fig. 4), Mesozoic granitic basement rocks are overlain unconformably by a series of thin (~2–5 m thick), dark-weathering, black, fine-grained, vesicular basalt and basaltic andesite flows with distinctive small (1 mm) olivine phenocrysts altered to bright reddish iddingsite(?) (unit Tob, Fig. 4). This unit is thickest (~350 m) south of Fisher Peak and thins and pinches out to the north and south (Fig. 4), indicating that it fills a small, roughly east-west–trending paleovalley that is now tilted down to the west.

A groundmass concentrate from the base of this unit west of Alta Creek Road (Fig. 4) yielded complex $^{40}Ar/^{39}Ar$ release spectra that do not define a plateau (Fig. 5). The two lowest-temperature steps are characterized by low radiogenic yields (<50%) and young ages; higher-temperature steps are highly radiogenic (90%–99%) and cluster about 30 Ma (Fig. 5). These steps yield a poorly defined isochron because of their low $^{36}Ar/^{40}Ar$ ratios; therefore, we calculate a weighted-mean age of 30.07 ± 0.40 Ma for these steps and consider this the best age for this sample (Fig. 5).

Tuffaceous Sedimentary Rocks and Ash-Flow Tuffs

The older basalts are overlain by as much as 400 m of thinly bedded, generally fine-grained, tuffaceous sedimentary rocks interbedded with ash-flow sheets and basalt flows. With the exception of densely welded ash flows and thin (<5 m) basalt flows, these poorly consolidated rocks are not well exposed and were mapped as a single unit (unit Ts, Fig. 4). Interbedded basalt flows extensive enough to be individually mapped are included in map unit Tob (Fig. 4). Two of the interbedded ash-flow tuffs (Tuff of Alder Creek and Ashdown Tuff) form important regional marker units and are described separately in following sections. The Tuff of Alder Creek is discontinuously exposed near the base of the sequence, and the Ashdown Tuff forms a distinctive, regionally extensive marker bed higher in the sequence (Figs. 3, 4). As much as 200 m of fine-grained tuffs and tuffaceous sedimentary rocks overlie the Ashdown Tuff, although the thickness of these rocks is difficult to measure because they are poorly exposed and disrupted by monoclinal folds and small normal faults (Fig. 4).

A groundmass concentrate from a thin basalt flow between the Alder Creek and Ashdown tuffs (sample PF13) yielded a $^{40}Ar/^{39}Ar$ plateau age of 26.20 ± 0.39 Ma (Fig. 5). Sanidine from an unnamed ash-flow tuff (sample PF17) a few meters above the Ashdown Tuff yielded a $^{40}Ar/^{39}Ar$ weighted-mean age of 25.27 ± 0.17 Ma (Fig. 5) from laser fusion of four multigrain aliquots (~1.2 mg each). A groundmass concentrate from a thin (~3 m thick) basalt flow higher in the section (sample PF21) yielded apparently flat $^{40}Ar/^{39}Ar$ release spectra at ca. 23.5 Ma that do not define a plateau because of the small uncertainties of individual heating steps (Fig. 5). We calculate a $^{40}Ar/^{39}Ar$ weighted-mean age of 23.65 ± 0.38 Ma on eight steps that make up >90% of the ^{39}Ar and consider this the best age for the sample (Fig. 5).

[1]GSA Data Repository item 2006013, Part 1—$^{40}Ar/^{39}Ar$ analytical data (text, tables, and graphics), Part 2—Fission-track-length data (text and graphics), Table DR3—Geochemical analysis of volcanic rocks from the Pine Forest Range, and Table DR4—Recalculated $^{40}Ar/^{39}Ar$ ages, is available on the Web at http://www.geosociety.org/pubs/ft2006.htm. Requests may also be sent to editing@geosociety.org.

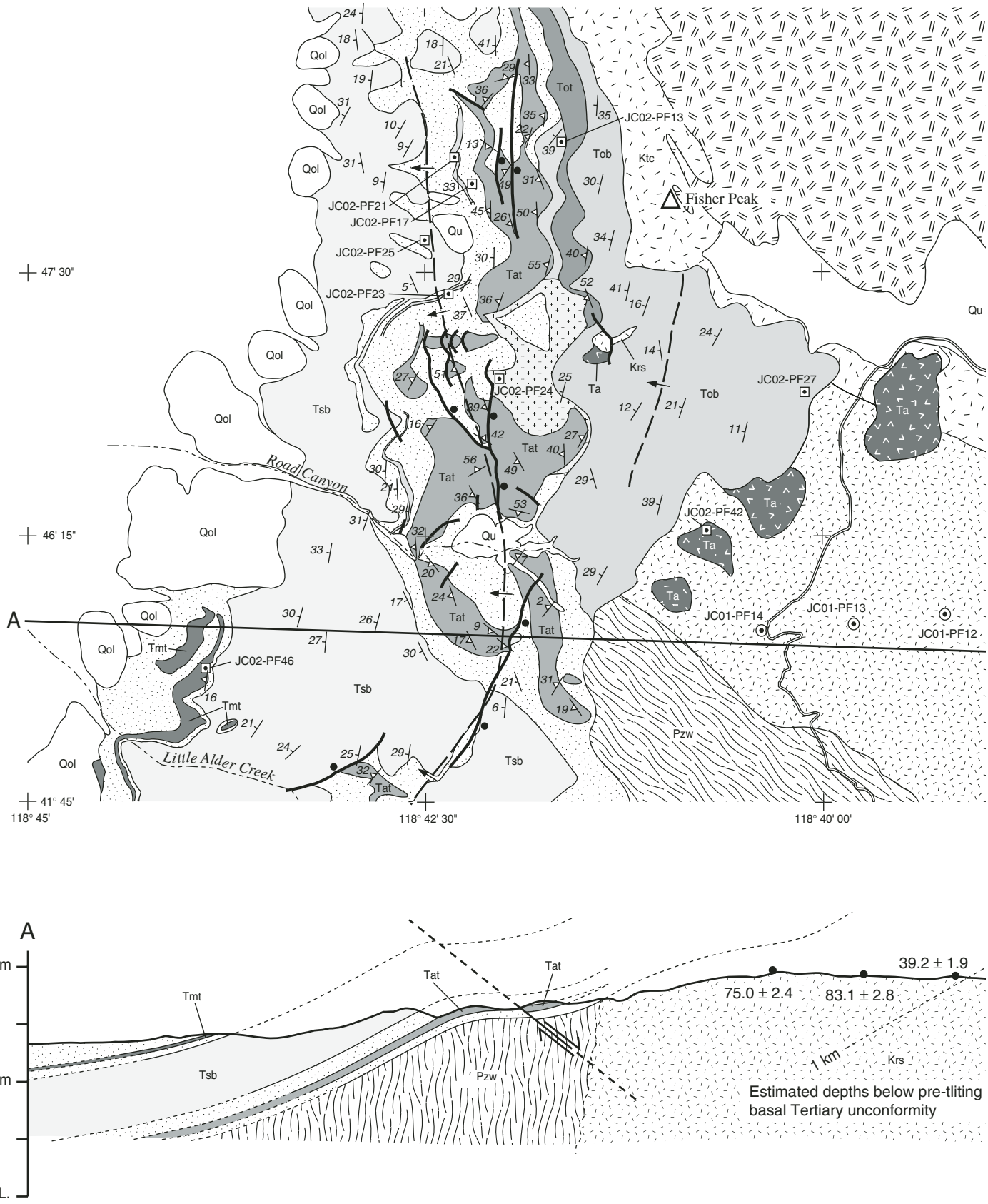

Figure 4. Geologic map and cross section of a part of northern Pine Forest Range. Distribution of Tertiary units from new mapping (1:24,000

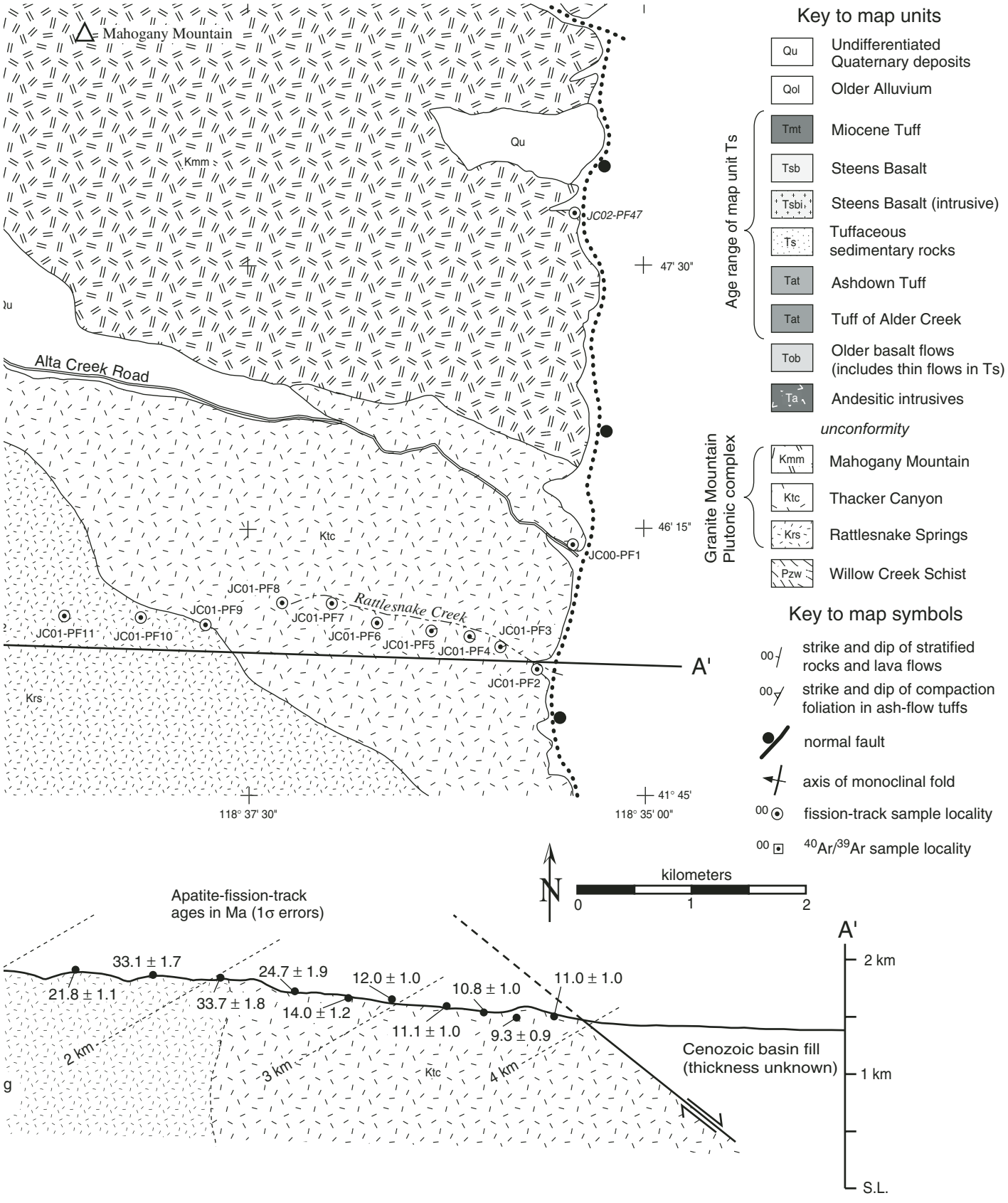

scale) by the authors; basement unit designations and contacts from Graichen (1972) and Wyld and Wright (2001). S.L.—sea level.

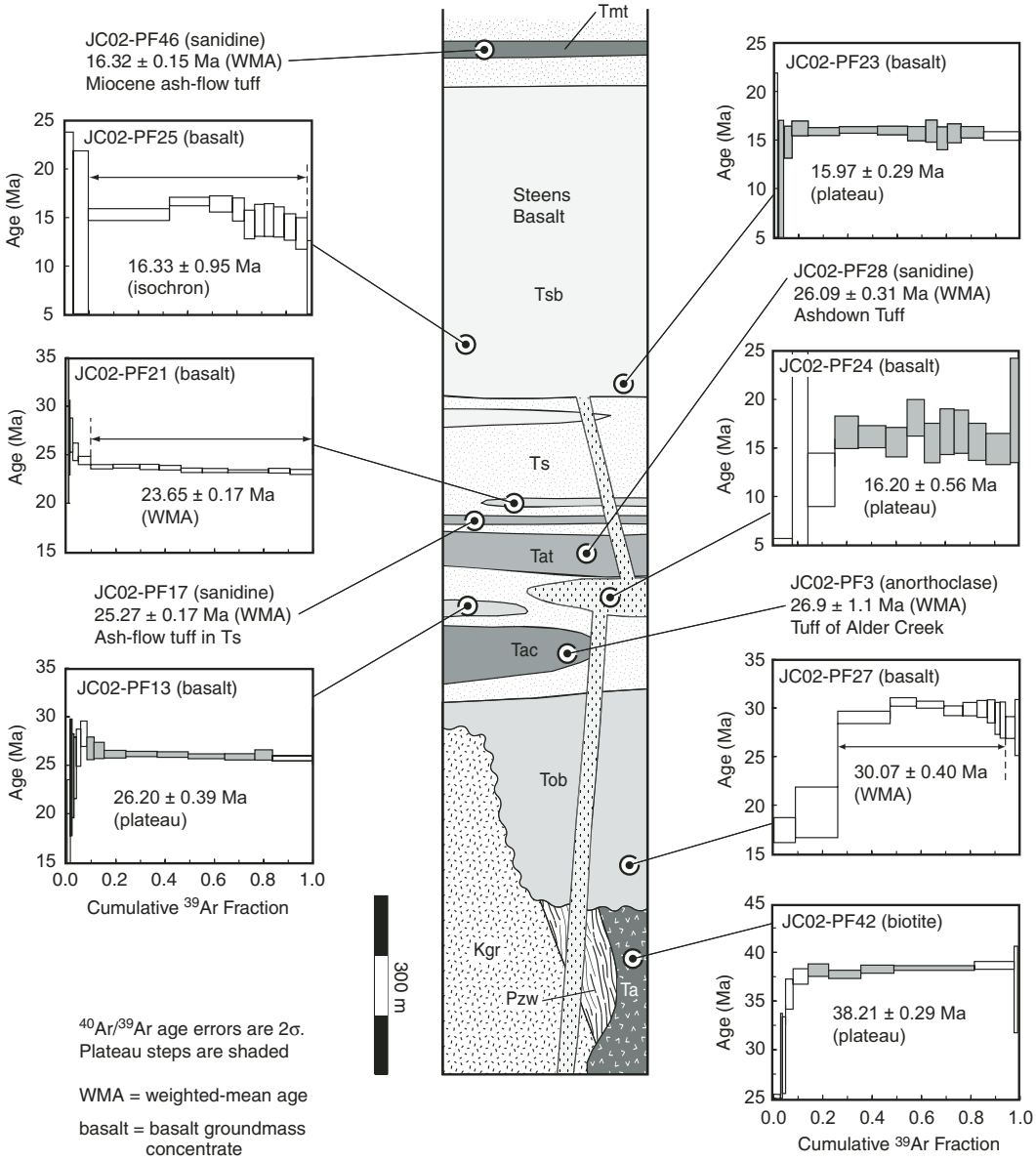

Figure 5. Schematic composite stratigraphic section of Tertiary units in northern Pine Forest Range, showing $^{40}Ar/^{39}Ar$ ages obtained in this study. Description of analytical procedures and complete age data are available in Data Repository item, Part 1 (see footnote 1).

Tuff of Alder Creek

The oldest mappable ash-flow tuff unit (unit Tac, Fig. 4) is a reddish-brown–weathering, pale orange-gray, densely welded trachydacitic ash-flow tuff that is relatively crystal poor and contains distinctive biotite and anorthoclase phenocrysts, with minor small (<1 cm) lithic fragments. We informally refer to this unit as the Tuff of Alder Creek after exposures just west of Alder Creek in the central part of the range (Fig. 3). The source area and regional distribution of the Tuff of Alder Creek are unknown, although it may be correlative with ash-flow tuffs in the Black Rock Range (Fig. 2) to the south, described by Lerch et al. (2004).

Four multigrain anorthoclase aliquots (~1.2 mg each) were analyzed by laser fusion from a sample of the Tuff of Alder Creek (sample PF3). Ages from these analyses yield a $^{40}Ar/^{39}Ar$ weighted-mean age of 26.9 ± 1.1 Ma but do not overlap at the 95% confidence level, ranging from 25.9 to 27.5 Ma. Inconsistency between analyses may result from contamination by older xenocrystic grains that would make 26.9 Ma a maximum age for this sample. The minimum age is constrained by the 26.20 ± 0.39 Ma age from an overlying basalt flow (sample PF13). Despite the uncertainty of these analyses, we assign the Tuff of Alder Creek an age of 26.9 ± 1.1 Ma, consistent with its stratigraphic position above sample PF27 (30.07 ± 0.40 Ma) and below sample PF13.

Ashdown Tuff

The Ashdown Tuff is the most widespread Tertiary unit in the northern Pine Forest Range and was named by Noble et al. (1970) for prominent exposures at the Ashdown Mine (Fig. 3). This unit is a distinctive, dark red–weathering, pale-reddish-gray, pumice- and crystal-rich alkali rhyolite ash-flow tuff. In the study area it is 20–50 m thick and densely welded, forming prominent dark-red cliffs that are an important marker for reconstructing Cenozoic faulting. It contains common lithic fragments up to ~1 cm in size; abundant, well-developed pumice fiamme; sparse biotite; and abundant sanidine phenocrysts that form distinctive,

TABLE 1. $^{40}Ar/^{39}Ar$ DATA

Sample number	Min.†	Map unit	Latitude (°N)	Longitude (°W)	Weighted-mean age (Ma)	Plateau age (Ma)	%^{39}Ar	Isochron age (Ma)	Comments
Ar-Ar step heating experiments									
JC02-PF25	bas	Tsb	41°46′10″	118°35′27″	15.77 ± 0.71	No plateau	89.3	16.33 ± 0.95	Steens Basalt
JC02-PF23	bas	Tsb	41°47′21″	118°42′13″		15.97 ± 0.29	83.5	16.07 ± 0.29	Steens Basalt
JC02-PF24	bas	Tsbi	41°47′01″	118°42′04″		16.20 ± 0.56	74.9	17.1 ± 1.8	Steens Basalt sill below Ashdown Tuff
JC02-PF21	bas	Tob	41°47′57″	118°42′18″	23.65 ± 0.17	No plateau	95.6	23.51 ± 0.45	Thin basalt flow above Ashdown Tuff
JC02-PF13	bas	Tob	41°48′01″	118°41′38″		26.20 ± 0.39	75.6	26.06 ± 0.42	Thin basalt flow below Ashdown Tuff
JC02-PF27	bas	Tob	41°46′48″	118°40′07″	30.07 ± 0.40	No plateau	68.5	29.59 ± 0.82	Oldest basalt flow in paleovalley
JC02-PF42	bio	Ta	41°46′12″	118°40′43″		38.21 ± 0.29	67.7	38.66 ± 0.37	Trachyandesite porphyry
Ar-Ar laser fusion experiments‡									
JC02-PF46	san	Tmt	41°46′18″	118°43′53″	16.32 ± 0.15	–	100	–	Tuff of Oregon Canyon? or Idaho Canyon?
JC02-PF17	san	Ts	41°47′56″	118°42′14″	25.27 ± 0.17	–	100	–	Ash-flow tuff above Ashdown Tuff
JC02-PF28	san	Tat	41°49′46″	118°42′01″	26.09 ± 0.31	–	100	–	Ashdown Tuff at Ashdown Mine
JC02-PF3	anc	Tac	41°49′46″	118°41′40″	26.9 ± 1.1	–	100	–	Tuff of Alder Creek, south of Ashdown Mine

Note: Preferred ages are used throughout the text. See Data Repository item, Part 1, for complete explanation of analytical procedures.
†Abbreviations: bas—basalt groundmass concentrate; bio—biotite; san—sanidine; anc—anorthoclase.
‡4–5 total fusion analyses of 3–6 grains each.

coarse-grained (>5 mm) euhedral crystals. The regional distribution and source of the Ashdown Tuff are unknown, although Noble et al. (1970) suggest a source in the Black Rock Range (Fig. 2) ~80 km to the south.

Noble et al. (1970) reported a K-Ar age of 25.1 ± 0.8 Ma on sanidine from the Ashdown Tuff (recalculated using decay constants of Steiger and Jäger, 1977). We analyzed five multigrain sanidine aliquots by laser fusion from a sample of the Ashdown Tuff (sample PF28) at its type locality at the Ashdown Mine (Fig. 3), which give a weighted-mean age of 26.09 ± 0.31 Ma (Fig. 5). This age is consistent with the stratigraphic position of the Ashdown Tuff above sample PF13 (26.20 ± 0.39 Ma) and below sample PF17 (25.27 ± 0.17 Ma). Our age is consistent with that of Swisher (1992), who obtained a $^{40}Ar/^{39}Ar$ age of 26.26 ± 0.03 Ma (TCs) for the Ashdown Tuff.

Steens Basalt

The older volcanic rocks are overlain by a thick (up to ~550 m) sequence of reddish-weathering, vesicular olivine basalt flows. These basalts were erupted locally from numerous north- to north-northwest–trending dikes and formed extensive sills within the Tertiary sedimentary section (Figs. 4, 5). Distinctive flows near the base of this unit contain >50% large tabular plagioclase phenocrysts (up to 4 cm long).

A groundmass concentrate from basaltic sills beneath the Ashdown Tuff southwest of Fisher Peak (sample PF24) yielded a $^{40}Ar/^{39}Ar$ plateau age of 16.20 ± 0.56 Ma (Fig. 5), confirming the relationship of the sills to the basalt flows higher in the section. A groundmass concentrate (sample PF25) from near the base of the basalt flows west of Fisher Peak (Fig. 4) yielded complex $^{40}Ar/^{39}Ar$ release spectra that do not define a plateau (Fig. 5). The 10 middle steps range from ca. 14–17 Ma (Fig. 5) and are characterized by low to moderate (40%–85%) radiogenic yields. Owing to the range of low radiogenic yields for these steps, we prefer the inverse-isochron age of 16.33 ± 0.95 Ma for this sample (Fig. 5). Another groundmass concentrate (sample PF23) from a thin flow near the base of the basalt section (Fig. 4) yielded a $^{40}Ar/^{39}Ar$ plateau age of 15.97 ± 0.29 Ma (Fig. 5). A minimum age for the basalt flows is given by the 16.32 ± 0.15 Ma age of an overlying tuff described in the next section (unit Tmt, Fig. 4). This age overlaps the three ages from the underlying basalts at the 95% confidence level. We therefore consider the basalt flows to be ca. 16.3 Ma, slightly older

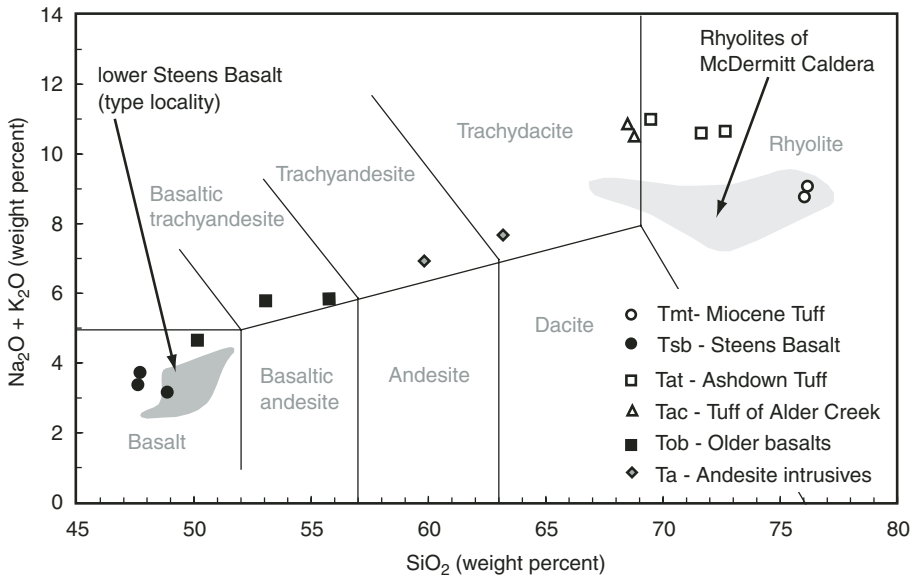

Figure 6. Total-alkali versus silica plot for Pine Forest Range volcanic rocks. Steens Basalt field from analyses of Johnson et al. (1998),"lower Steens" subdivision from Camp et al. (2003). McDermitt Rhyolite field from analyses of Rytuba and McKee (1984). Field lines and rock names after Le Maitre et al. (1989). Complete major-element data available in Table DR3 (see footnote 1).

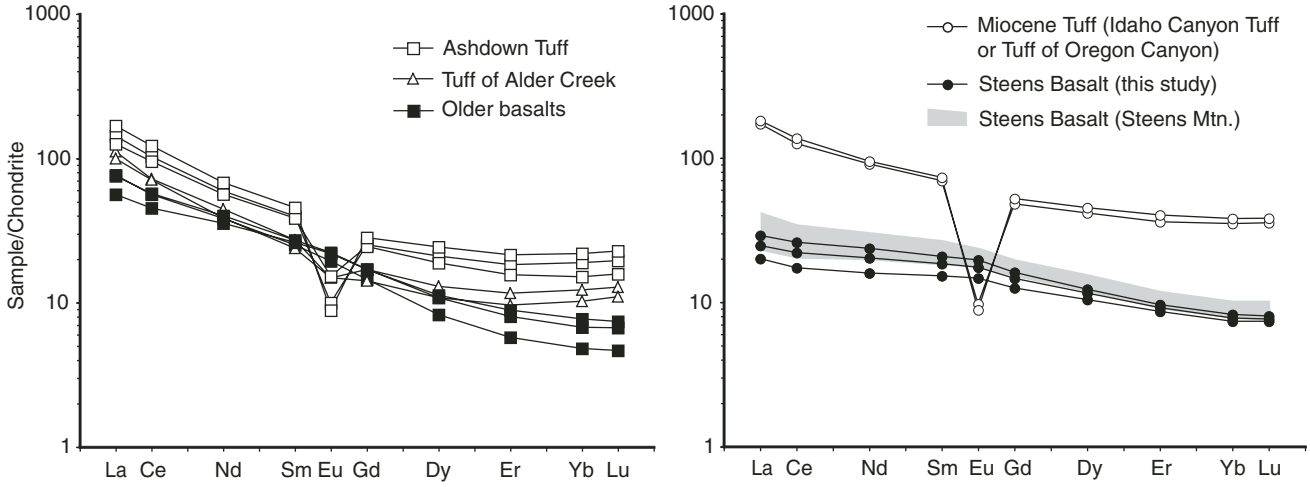

Figure 7. Rare-earth-element plots for Pine Forest Range volcanic rocks. Data are chondrite normalized (Masuda et al., 1973). Steens Basalt field from Johnson et al. (1998). Complete trace-element data available in Table DR3 (see footnote 1).

than the overlying tuff but statistically indistinguishable from it on the basis of these data.

On the basis of similar petrographic character, age, and geochemistry, we correlate these basalt flows with the regionally extensive Steens Basalt, which has been mapped along strike to the north in the Pueblo Mountains (Roback et al., 1987; Hart et al., 1989). The dark, coarsely plagioclase-phyric flows near the base of the section are similar to flows in the lower part of the Steens Basalt at its type locality at Steens Mountain (Fig. 2) (Johnson et al., 1998). Swisher (1992) obtained $^{40}Ar/^{39}Ar$ ages of 16.41 ± 0.02 Ma (TCs) (base) and 16.40 ± 0.05 Ma (TCs) (top) for the Steens Basalt at Steens Mountain, within the larger uncertainty of our ca. 16.3 Ma estimate for its age in the Pine Forest Range. Although geochemical data were collected for only three samples of this unit, the data are similar to analyses of the lower Steens Basalt at Steens Mountain (as subdivided by Camp et al., 2003), analyzed by Johnson et al. (1998) (Fig. 6).

Miocene Tuff

The youngest dated unit is a thin (<30 m) dark-red–weathering, blue-gray to blue-green, densely welded rhyolite ash flow that crops out in the southwestern part of the study area (unit Tmt in Fig. 4). It contains rare angular lithic fragments, abundant pumice, and common euhedral sanidine phenocrysts.

Sanidine from this unit (sample PF46) yielded a $^{40}Ar/^{39}Ar$ weighted-mean age of 16.32 ± 0.15 Ma (Fig. 5) from laser-fusion analyses of four multigrain aliquots (~1.2 mg each). On the basis of age and composition, we consider two potential correlations—source areas for this tuff—but are unable to distinguish between them: the Tuff of Oregon Canyon (Rytuba and McKee, 1984) or the Idaho Canyon Tuff (Noble et al., 1970).

The Tuff of Oregon Canyon erupted from the McDermitt Caldera to the east (Fig. 2) and directly overlies exposures of the Steens Basalt along strike to the north in the Pueblo Mountains (Fig. 2) (Rytuba and McKee, 1984; Roback et al., 1987). The Tuff of Oregon Canyon is similar in composition, appearance, and geochemistry to the tuff described here, and Rytuba and McKee (1984) dated it at 16.1 ± 0.2 Ma (K-Ar sanidine), within the uncertainty of our 16.32 ± 0.15 Ma age.

The other likely correlation for this tuff is the Idaho Canyon Tuff (Noble et al., 1970), erupted from the nearby Virgin Valley Caldera to the west (Fig. 2; Castor and Henry, 2000). The Idaho Canyon Tuff is similar in composition and appearance to the tuff described here, and Swisher (1992) obtained a $^{40}Ar/^{39}Ar$ age of 16.30 ± 0.04 Ma (TCs) for the former that agrees well with our 16.32 ± 0.15 Ma determination, although Castor and Henry (2000) obtained a slightly younger age of 16.12 ± 0.06 Ma (TCs) for the same tuff.

GEOCHEMISTRY

Major- and trace-element geochemical data were obtained from 15 samples to characterize the rocks described previously, but detailed petrogenetic analysis of this suite of rocks is beyond the scope of this paper. The data are primarily intended to properly name these rocks and illustrate the bimodal nature of both the Oligocene (ca. 30–23 Ma) and Miocene (ca. 17–16 Ma) volcanic sequences (Figs. 5, 6).

The 38 Ma intrusive rocks are trachyandesitic (Fig. 6) and thus distinctly different from the overlying Oligocene and Miocene basalts and rhyolites. These intrusions may be related to development of the Eocene Cascade magmatic arc in northwestern Nevada (discussed in Christiansen and Yeats, 1992) or to the earliest stages of the major magmatic activity that swept across central Nevada during Eocene–Oligocene time (e.g., Armstrong and Ward, 1991), but the sparse outcrop of these units and the limited data obtained in this study preclude a more detailed analysis.

Both the Oligocene (30–23 Ma) and Miocene (17–16 Ma) volcanic suites are bimodal, but the Oligocene rocks are mostly trachytic and range more widely in silica content, from basalt and basaltic andesite to dacite and rhyolite (Fig. 6), whereas the Miocene (ca. 17–16 Ma) rocks consist only of true basalt and rhyolite (Fig. 6). Too little geochemical data are available to address the significance of these differences, but they may indicate that Oligocene magmas were generated from a different source that interacted to a different degree with underlying crust than the Miocene magmas.

TERTIARY NORMAL FAULTING AND TILTING

Previous workers mapped an unconformity in the northern Pine Forest Range Tertiary section (Graichen, 1972). Noble et al. (1970) describe

"progressive offlap relations and angular discordance" between the 26 Ma Ashdown Tuff and the 16 Ma Tuff of Craine Creek to the south of our study area, although the precise location of this relationship is not specified. A major goal of this study was to determine if there is evidence for extensional faulting and tilting of the volcanic rocks prior to the high-angle faulting that formed the modern Pine Forest Range.

Geologic mapping (1:24,000 scale) in the Vicksburg Canyon Quadrangle (Fig. 4) demonstrates that the Tertiary volcanic section is everywhere conformable (with the exception of the early intrusives) and that variations in the dip of Tertiary rocks result from bending related to small-offset normal faults (shown in cross section A–A′, Fig. 4). Although these bends locally give the appearance of angular discordance between the Ashdown Tuff and the younger Steens Basalt, the west dip of the entire section varies from near horizontal to 35°–40°, and there is no systematic variation with age, indicating that bending postdates the youngest (16.3 Ma) units.

The modern Pine Forest Range is bounded to the east by an east-dipping, down-to-the-east normal fault that accommodated uplift and tilting of the modern range (Figs. 3, 4). The northern part of the range is tilted as an intact block along this fault. To the south, the interior of the range is broken by two other north-striking faults, the Leonard Creek and Alder Creek Faults (Fig. 3). In the northern part of the range, dip-slip motion on the range-front fault resulted in at least 2.5 km of vertical offset (Fig. 4), but no direct (e.g., seismic or borehole) data are available for determining the depth of the basin fill in the adjacent valley. Basin-depth maps (1:2,500,000 scale) from gravity data (Saltus and Jachens, 1995) suggest that sedimentary fill in this valley is no thicker than 0.5–1.0 km, indicating a minimum of 3–3.5 km vertical offset for the range-front fault.

Where exposed at Four Springs (Fig. 3), the range-front fault dips ~40°E, with well-developed striations indicating dip-slip motion (Fig. 3). We infer that the Pine Forest Range was tilted up to 30°–35° during a single episode of extensional movement along this fault, which originally would have dipped ~70°E. The amount of tilting varies along strike from ~20° in the southern part of the range to ~40° near the Ashdown Mine to the north (Fig. 3). In the southern part of the range (Fig. 3), extension was taken up by three faults, with correspondingly less rotation of the footwall blocks. To the north, extension and tilting took place along a single fault (Fig. 3), leading to a greater amount of rotation and tilting to accommodate the same amount of horizontal extension. Along the line of section A–A′ (Fig. 4), 30° tilting of the range resulted in ~5–6 km of horizontal extension, although the absence of robust constraints on the depth to basement east of the range-front fault makes this a relatively crude estimate.

FISSION-TRACK DATING OF PINE FOREST RANGE UPLIFT

The fission-track method is routinely used to date the timing of slip on major normal fault systems in many parts of the Basin and Range province (e.g., Fitzgerald et al., 1991; Stockli et al., 2003; Surpless et al., 2002; Armstrong et al., 2003), and a detailed explanation of this application is given in Miller et al. (1999). Apatite fission-track ages are reset to zero age at subsurface temperatures >~110–135 °C, generally equivalent to subsurface depths >~3–5 km. Ages are partially reset over the temperature range ~60–110 °C, termed the partial annealing zone (PAZ) (e.g., Green et al., 1989; Dumitru, 2000). Broader track-length distributions and shorter mean track lengths are characteristic of longer residence time in the PAZ, whereas consistently longer tracks indicate relatively rapid cooling through the temperature interval ~110–60 °C (e.g., Gleadow et al., 1986; Green et al., 1989). To determine the time of slip on major normal faults, systematic transects of samples were collected across the footwall of the fault system to obtain samples that resided at the widest possible range of paleodepths—and thus paleotemperatures—before extension and exhumation began.

Seventeen fission-track samples were analyzed from the Pine Forest Range (Table 2), fourteen from an east-west transect (Figs. 3, 4) across the Granite Mountain plutonic complex, two from the range front north and south of the transect (Fig. 3), and 1 additional sample from the base of New York Peak along the Leonard Creek Fault to the south and west (Fig. 3). In general, the samples from the Rattlesnake Springs and Thacker Canyon phases of the Granite Mountain plutonic complex (Fig. 4) yielded abundant, high-quality apatite, whereas apatite from the Mahogany Mountain quartz monzonite and the granodiorite underlying New York Peak (Fig. 3) was generally of lower quality (fewer grains, more fractures and dislocations).

To calculate the pre-extensional paleodepths of samples shown in Figure 8, we projected the basal Tertiary unconformity across the range with a dip of 30° along line A–A′ (Fig. 4) and added the present thickness of the volcanic rocks along line A–A′ (~1100 m) to the vertical depth of each sample beneath the unconformity. In doing so, we assumed that no faults or folds disrupt the basement rocks east of the oldest Tertiary rocks (Fig. 3). Previous workers (Smith, 1973; Wyld, 1996) did not map any fault offset of the gradational contact between the Rattlesnake Springs and Thacker Canyon plutons, and no evidence of faulting was observed along the line of the fission-track sample transect.

The Pine Forest Range fission-track ages exhibit a systematic decrease with increasing structural depth, as expected in an exhumed normal-fault footwall block (Fig. 8A, B). At shallow structural depths, 83–75 Ma ages and long track lengths record an older cooling event unrelated to extensional faulting. At intermediate depths (~1.8–3.9 km), ages trend progressively younger (Fig. 8A) and track lengths trend shorter (Fig. 8B), reflecting incomplete resetting of the fission-track system within the PAZ before exhumation began. At paleodepths deeper than ~4 km, samples have nearly uniformly young apparent ages and longer track lengths, indicating that they were fully reset to zero age (hotter than ~110 °C) prior to exhumation and cooling through the PAZ.

The data define an exhumed pre-extensional fission-track PAZ, the base of which (110 ± 10 °C) lies at 3.9 ± 0.1 km paleodepth (Fig. 8). Samples below this depth have mostly long tracks (~14 μm) indicative of relatively rapid cooling through the PAZ, whereas samples directly above this depth have shorter mean track lengths (12–13 μm) and broader distributions of track lengths resulting from longer residence time in the PAZ (Fig. 8). The top of the exhumed PAZ (60 ± 5 °C) lies at ~1.8 ± 0.2 km paleodepth; above this level, samples preserve Cretaceous ages unreset prior to Cenozoic faulting (Fig. 8). Assuming a surface temperature of 10 ± 5 °C, the position of the exhumed PAZ is consistent with a pre-extensional (late Miocene) geothermal gradient of 26 ± 6 °C/km.

Older (83–75 Ma) samples from above the PAZ date an earlier event unrelated to extensional faulting, possibly regional exhumation of this region during the Late Cretaceous–Early Tertiary. Samples within the PAZ trend progressively younger overall, but sample PF11 is anomalously young, with long track lengths indicative of rapid cooling (Fig. 8). Numerous thin (~0.5–2 m), undated mafic dikes intrude the granitic basement along the fission-track sample transect and are presumed to be coeval with either Oligocene or middle Miocene volcanism. We interpret sample PF11 as partially reset by localized heating associated with Tertiary dike emplacement, because it appears to have rapidly cooled at a time corresponding to no known structural or regional tectonic event.

The structurally deepest samples from beneath the PAZ (close to the range front) document tilting, uplift, and cooling of the range ca. 11–7 Ma.

TABLE 2. FISSION-TRACK SAMPLE LOCALITY, COUNTING, AND AGE DATA

Sample number	Irradiation number	Latitude (°N)	Longitude (°W)	Est. PD (m)	No. Xls	Spontaneous		Induced		P(c^2) (%)	Dosimeter		Age ± 1s (Ma)
						Rho-S	NS	Rho-I	NI		Rho-D	ND	
JC00-PF1	SU055–19	41°46′10″	118°35′27″	4910	35	0.0326	63	1.0069	1944	44.7	1.4729	3877	8.8 ± 1.1
JC01-PF2	SU058–01	41°45′36″	118°35′41″	4880	36	0.0597	130	1.3635	2969	36.2	1.3743	4065	11.0 ± 1.0
JC01-PF3	SU058–02	41°45′42″	118°35′54″	4730	35	0.0386	113	1.0563	3095	25.3	1.3818	4065	9.3 ± 1.0
JC01-PF4	SU058–03	41°45′45″	118°36′06″	4540	35	0.0485	156	1.1313	3638	17.2	1.3818	4065	10.8 ± 1.0
JC01-PF5	SU058–04	41°45′47″	118°36′21″	4340	35	0.0479	139	1.1090	3217	48.7	1.3967	4065	11.1 ± 1.0
JC01-PF6	SU058–05	41°45′49″	118°36′41″	4060	35	0.0631	179	1.3521	3838	56.8	1.3967	4065	12.0 ± 1.0
JC01-PF7	SU058–06	41°45′55″	118°36′58″	3840	35	0.0631	146	1.1713	2710	72.5	1.4116	4065	14.0 ± 1.2
JC01-PF8	SU058–07	41°45′55″	118°37′17″	3570	35	0.0949	208	0.9945	2179	15.8	1.4116	4065	24.7 ± 1.9
JC01-PF9	SU058–08	41°45′49″	118°37′46″	3110	35	0.2896	598	2.2516	4649	15.4	1.4264	4065	33.7 ± 1.8
JC01-PF10	SU058–09	41°45′51″	118°38′11″	2810	35	0.2697	474	2.1342	3751	34.9	1.4264	4065	33.1 ± 1.7
JC01-PF11	SU058–10	41°45′51″	118°38′40″	2420	30	0.2920	578	3.5464	7019	77.8	1.4413	4065	21.8 ± 1.1
JC01-PF12	SU058–12	41°45′53″	118°39′14″	2040	30	0.4287	741	2.8998	5012	35.2	1.4488	4065	39.2 ± 1.9
JC01-PF13	SU058–13	41°45′51″	118°39′48″	1620	31	1.1561	2223	3.7185	7150	31.2	1.4637	4065	83.1 ± 2.8
JC01-PF14	SU058–14	41°45′49″	118°40′23″	1330	25	1.8266	3118	6.5541	11188	0.4	1.4637	4065	75.0 ± 2.4
JC02-PF44	SU059–06	41°34′00″	118°45′20″	1500	23	1.6828	849	5.4526	2751	18.9	1.4040	4095	79.3 ± 4.0
JC02-PF47	SU059–07	41°47′47″	118°35′28″	5210	35	0.0425	60	1.6103	2273	1.1	1.4125	4095	7.3 ± 1.0
JC02-PF48	SU059–08	41°43′47″	118°35′12″	5370	35	0.0754	110	2.8126	4104	8.8	1.4125	4095	7.0 ± 0.7

Note: Abbreviations: Est. PD—estimated sample paleodepth, meters; No. Xls—number of individual crystals (grains) dated; Rho-S—spontaneous track density (×106 tracks per cm^2); NS—number of spontaneous tracks counted; Rho-I—induced track density in external detector (muscovite) (×106 tracks per cm^2); NI—number of induced tracks counted; P(c^2)—c^2 probability (Galbraith, 1981; Green, 1981); Rho-D—induced track density in external detector adjacent to dosimetry glass (×106 tracks per cm^2); ND—number of tracks counted in determining Rho-D. Age is the sample central-fission-track age (Galbraith and Laslett, 1993), calculated using zeta calibration method (Hurford and Green, 1983) with a zeta factor of 367.6 ± 5.0. Analyst: J.P. Colgan.

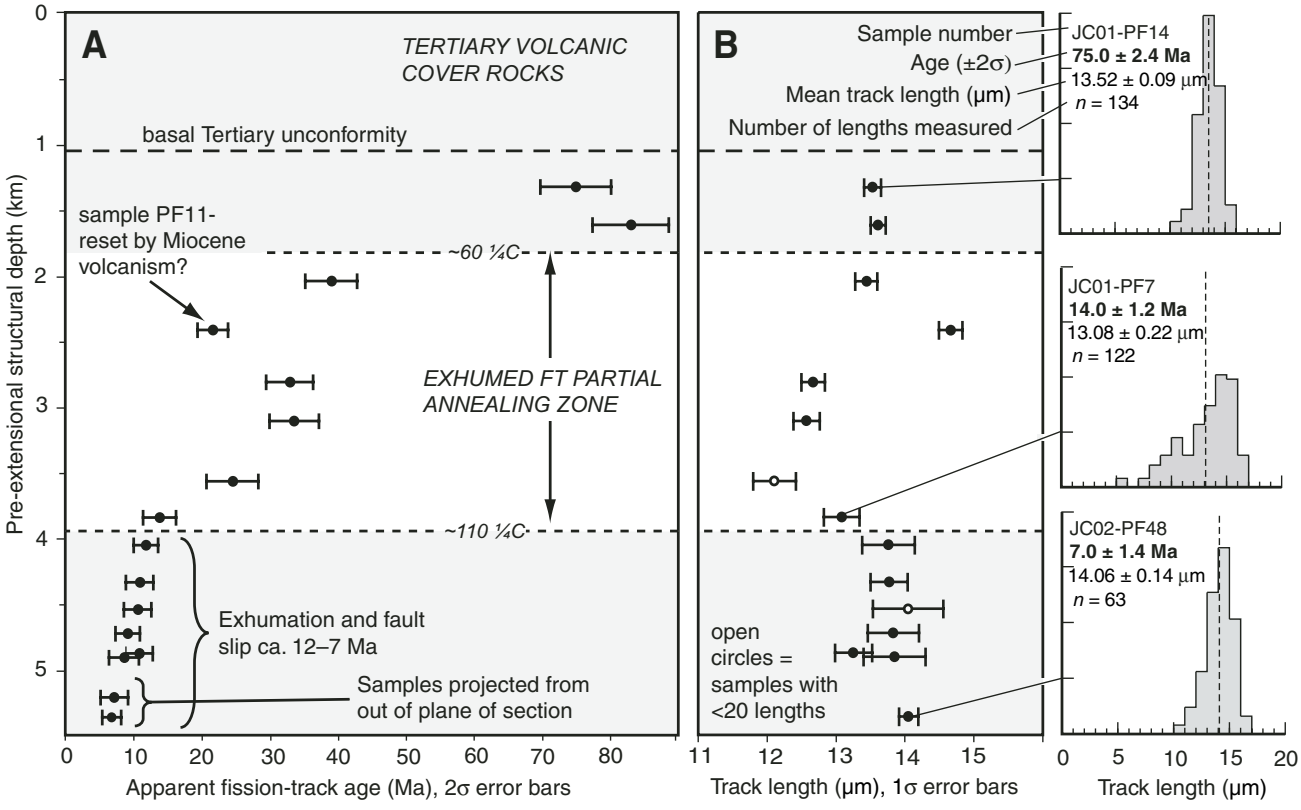

Figure 8. Age and length data for Pine Forest Range fission-track samples. (A) Age versus paleodepth plot. (B) Mean track length versus paleodepth plot. Also shown are three representative track-length histograms from above, within, and below the partial annealing zone. Complete age data shown in Table 1; complete length data and description of analytical procedures available in Data Repository item, Part 2 (see footnote 1). FT—Fission-track.

The precise onset of faulting is difficult to pinpoint with this data set, but it probably began ca. 12–11 Ma. The youngest sample along the main transect is 8.8 Ma, and additional samples from slightly deeper paleodepths to both the north and south of the main transect (Fig. 3) have apparent ages of ca. 7 Ma, indicating that faulting and uplift of the range were ongoing ca. 11–7 Ma. The amount of post–7 Ma fault slip and uplift is not known, but it was not sufficient to exhume younger fission-track ages and was therefore probably <2 km (equivalent to subsurface temperatures of ~60 °C). Although no historic earthquakes have occurred in the Pine Forest Range, and there is no obvious evidence (e.g., fault scarps in alluvium) for historic slip on the range-bounding fault, well-developed triangular facets on the east side of the range suggest at least some offset along this fault within the past million years.

DISCUSSION

Late Cretaceous–Early Tertiary Cooling

Late Cretaceous fission-track ages from the structurally highest level of the pre-Tertiary basement in the northern Pine Forest Range (within 500 m of the basal Tertiary unconformity) indicate that the area was exhumed to within a few kilometers of the surface by 83–75 Ma and has not been buried significantly (greater than subsurface depths equivalent to ~60 °C) since that time. Exposure of ca. 38 Ma intrusive bodies prior to deposition of the oldest (30 Ma) Tertiary lava flows further testify to at least some erosion and development of topographic relief on the exposed Mesozoic-Paleozoic basement surface during the late Eocene–early Oligocene. The absence of mapped Eocene volcanic rocks in northwestern Nevada makes it difficult to estimate the thickness of material eroded during this time, but the amount of overburden was not sufficient to reset Cretaceous fission-track ages from the underlying basement, and therefore the eroded material was probably <1–2 km thick.

Oligocene Volcanism

Beginning ca. 30 Ma, older topography in the northern Pine Forest Range was filled and covered by basalt flows and ash-flow tuffs erupted in the Oligocene. Although the source areas of these eruptions are not known, thick (>1 km) sequences of Oligocene basalts and ash-flow tuffs crop out to the south in the Black Rock Range and Calico Hills (Noble et al., 1970; Lerch et al., 2004) and, to a lesser degree, to the north in the Pueblo Mountains (Roback et al., 1987) (Fig. 2). Ash-flow tuffs similar in age (26–25 Ma) to those in the Pine Forest Range also crop out to the west in the Warner Range (Fig. 2) (Duffield and McKee, 1986); thus, late Oligocene volcanism in the northern Pine Forest Range appears to have been part of a more regionally extensive episode of bimodal volcanism.

Oligocene volcanic rocks in the Pine Forest Range were erupted over the same interval as the extensive series of ash-flow tuffs erupted across much of central Nevada between 43 and 17 Ma (e.g., Stewart, 1980), with the greatest volume having erupted between 31 and 20 Ma (Best and Christiansen, 1991). However, the bimodal, alkalic composition of the Pine Forest Range rocks distinguishes them from the great volume of ignimbrites erupted to the south and east, which are predominantly calc-alkaline and more intermediate in composition (e.g., Christiansen and Lipman, 1972; Best and Christiansen, 1991).

Voluminous Eocene–early Miocene calc-alkaline volcanism in the Basin and Range is commonly thought to have resulted from progressive-southward removal or decoupling of the shallowly subducting Farallon slab and the resulting influx of hot asthenospheric material into the crust (e.g., Humphreys, 1995), causing "belts" of magmatism to sweep southward across the Basin and Range (e.g., Armstrong and Ward, 1991). Widespread intermediate volcanism across much of Nevada during this time (Fig. 1) resulted from mixing of basalt with continental crustal material. The initial basalts may have been trapped in thickened, warm, unextending crust (e.g., Best and Christiansen, 1991) or mixed into a ductily flowing lower crust during rapid extension (e.g., Gans et al., 1989).

If Oligocene volcanism in northwestern Nevada was fed by the same asthenospheric upwelling as the central Nevada "ignimbrite flareup," why were the erupted volcanic rocks more bimodal than calc-alkaline? Basaltic magmas may have risen more easily through an initially thinner crust than that in central Nevada, where the crust was thickened to at least 50 km by the end of the Cretaceous (e.g., Coney and Harms, 1984). The crust beneath northwestern Nevada is composed of Phanerozoic volcanic arc terranes intruded by Cretaceous granitic plutons. Both the Paleozoic arc rocks and the mafic roots that likely underlie the granitic plutons are potentially more refractory than the thrust-thickened miogeoclinal strata that underlie much of central and eastern Nevada (e.g., Stewart, 1978) and thus are prone to a lesser degree of partial melting when intruded by basalts. Finally, the amount of basalt initially added to the crust may simply have been smaller in northwestern Nevada than in central Nevada, with correspondingly less ability to melt and assimilate continental crust. Although all of these factors are plausible, more detailed regional geologic and geochemical studies are necessary to determine why Oligocene volcanism proceeded differently in northwestern Nevada than it did in most other parts of the Basin and Range.

Timing of Extensional Faulting

Following the eruption of 30–23 Ma volcanic rocks, northwestern Nevada was volcanically inactive until the eruption of the Steens Basalt, beginning ca. 16.5 Ma. The Steens Basalt is equivalent to, but slightly older than, the more voluminous Columbia River basalts to the north (Fig. 1) and may represent the earliest eruptions of the larger Columbia River flood basalt province (Hooper et al., 2002). Many workers consider these flood basalts to have resulted from initial mid-Miocene impingement of the voluminous deep mantle plume that underlies the modern Yellowstone hotspot (e.g., Pierce and Morgan, 1992; Camp et al., 2003), although a mantle plume origin for both the basalt eruptions and the Yellowstone hotspot itself remains controversial (e.g., Christiansen et al., 2002; Foulger et al., 2004). Whatever their source, these eruptions are impressive both in volume (up to 300,000 km^3) and eruption rate, with >90% of the total volume having erupted between 16.1 and 15.0 Ma (Hooper et al., 2002). They thus form an important regional stratigraphic marker that is useful for reconstructing Basin and Range faulting.

In the Pine Forest Range, the Steens Basalt is conformable with the underlying Oligocene volcanic rocks and is tilted up to 30°–35°, demonstrating that the area was unbroken by large-offset normal faults during the interval 30–17 Ma. Similar geologic relationships exist in the Black Rock Range (Fig. 2), where 35–23 Ma basalts and rhyolites dip gently (<10°) and are conformable with overlying 16 Ma and younger ash-flow tuffs (Lerch et al., 2004); the Warner Range (Fig. 2), where Duffield and McKee (1986) documented a conformable 34–14 Ma sequence of volcanic rocks that dip ~25°W; and the Pueblo Mountains (Fig. 2), where the Steens Basalt dips ~20°W and conformably overlies a small volume of Oligocene rocks mapped by Roback et al. (1987). In the Bilk Creek Mountains, just east of the Pine Forest Range (Fig. 2), the Steens Basalt and overlying ash-flow tuffs are cut by multiple faults and dip 20°–30° (Minor, 1986). Farther east in the Santa Rosa Range (Fig. 2), 16.5–15 Ma mafic lavas unconformably overlie pre-Tertiary basement and dip gently (~15°) to the east (Brueseke et al., 2003), and apatite fission-track data (Colgan et al., 2004) argue against faulting and tilting prior to deposition of these rocks. These relationships suggest that a

potentially large region of northwestern Nevada (up to ~10,000 km^2 after regional extension) remained intact and unextended during peak Oligocene and middle Miocene volcanism, including the region between the Pine Forest and Warner Ranges now covered by flat-lying, ca. 16.5 Ma and younger volcanic rocks.

Apatite fission-track data from the Pine Forest Range are consistent with geologic evidence for post–16 Ma faulting and tilting, and they demonstrate that extensional faulting and uplift of the modern Pine Forest Range along high-angle faults began as early as ca. 12–11 Ma and was ongoing from 10 to 7 Ma. Fission-track ages and geologic relationships from the Santa Rosa Range (Fig. 2) to the east also indicate a 10–6 Ma age for extensional faulting (Colgan et al., 2004), and Duffield and McKee (1986) suggest a <14 Ma age for the onset of faulting in the Warner Range (Fig. 2). Thus it appears that the Basin and Range province in the region between the Warner and Santa Rosa Ranges (Fig. 2) developed during late Miocene time in a region of previously little extended crust.

CONCLUSIONS

The preservation of Cretaceous fission-track ages from high structural levels of the Pine Forest Range footwall block testifies to modest erosion and development of topographic relief on the pre-Tertiary basement surface during the Late Cretaceous–early Oligocene. Oligocene (30–23 Ma) bimodal volcanic rocks are conformably overlain by a younger Miocene (17–16 Ma) basalt-rhyolite suite on the west side of the range, demonstrating that no significant faulting and tilting took place between 30 and 16 Ma. Oligocene and Miocene volcanic rocks were tilted up to ~30°–35° during later Basin and Range extension and high-angle faulting that began ca. 12–11 Ma and was ongoing ca. 10–7 Ma. These data indicate that Basin and Range faulting in northwestern Nevada is distinctly younger and of lower total magnitude than that in central and eastern Nevada, where multiple generations of large offset faults were active from the Eocene into the middle Miocene.

ACKNOWLEDGMENTS

This project was supported by Geological Society of America graduate research grants, the Stanford University McGee Fund, the American Chemical Society Petroleum Research Fund Grant 39063-AC8 (to E.L. Miller), and U.S. National Science Foundation grant EAR-0229854 (to E.L. Miller), and EAR-0346245 (to S.L. Klemperer). Descriptions of the volcanic rocks benefited from discussions with D.A. John and G.A. Mahood. We thank the Oregon State University Radiation Center for sample irradiations and Win-Eldrich Mines, Ltd., for access to the Ashdown Mine site. Reviews by Chris Henry and Matt Heizler significantly improved presentation of the $^{40}Ar/^{39}Ar$ ages reported here.

REFERENCES CITED

Armstrong, P.A., Ehlers, T.A., Chapman, D.S., Farley, K.A., and Kamp, P.J., 2003, Exhumation of the central Wasatch Mountains, Utah: 1. Patterns and timing of exhumation deduced from low-temperature thermochronology data: Journal of Geophysical Research, v. 108, B3, 2172, doi:10.1029/2001JB001708.

Armstrong, R.L., and Ward, P.L., 1991, Evolving geographic patterns of Cenozoic magmatism in the North American Cordillera: The temporal and spatial association of magmatism and metamorphic core complexes: Journal of Geophysical Research, v. 96, p. 13,201–13,224.

Best, M.G., and Christiansen, E.H., 1991, Limited extension during peak Tertiary volcanism, Great Basin of Nevada and Utah: Journal of Geophysical Research, v. 96, p. 13,509–13,528.

Brueseke, M.E., Hart, W.K., Wallace, A.R., Heizler, M.T., and Fleck, R.J., 2003, Mid-Miocene volcanic field development in northern Nevada: New age constraints on the timing of Santa Rosa–Calico volcanism: Geological Society of America Abstracts with Programs, v. 35, no. 4, p. 63.

Bryant, G.T., 1970, The general geology of the northernmost part of the Pine Forest Mountains, Humboldt County, Nevada [M.S. thesis]: Corvallis, Oregon State University, 75 p.

Camp, V.E., Ross, M.E., and Hanson, W.E., 2003, Genesis of flood basalts and Basin and Range volcanic rocks from Steens Mountain to the Malheur River Gorge, Oregon: Geological Society of America Bulletin, v. 115, p. 105–128, doi: 10.1130/0016-7606(2003)1152.0.CO;2.

Castor, S.B., and Henry, C.D., 2000, Geology, geochemistry, and origin of volcanic rock–hosted uranium deposits in northwestern Nevada and southeastern Oregon, USA: Ore Geology Reviews, v. 16, p. 1–40, doi: 10.1016/S0169-1368(99)00021-9.

Christiansen, R.L., and Lipman, P.W., 1972, Cenozoic volcanism and plate-tectonic evolution of the western United States; I, Early and middle Cenozoic: Philosophical Transactions of the Royal Society of London, Ser. A, Mathematical and Physical Sciences, v. 271, p. 217–248.

Christiansen, R.L., and Yeats, R.S., 1992, Post-Laramide geology of the U.S. Cordilleran region, *in* Burchfiel, B.C., et al., eds., The Cordilleran orogen: Conterminous U.S.: Boulder, Colorado, Geological Society of America, Geology of North America, v. G-3, p. 261–406.

Christiansen, R.L., Foulger, G.R., and Evans, J.R., 2002, Upper-mantle origin of the Yellowstone hotspot: Geological Society of America Bulletin, v. 114, p. 1245–1256, doi: 10.1130/0016-7606(2002)1142.0.CO;2.

Colgan, J.P., Dumitru, T.A., and Miller, E.L., 2004, Diachroneity of Basin and Range extension and Yellowstone hotspot volcanism in northwestern Nevada: Geology, v. 32, p. 121–124, doi: 10.1130/G20037.1.

Coney, P.J., and Harms, T.A., 1984, Cordilleran metamorphic core complexes; Cenozoic extensional relics of Mesozoic compression: Geology, v. 12, p. 550–554, doi: 10.1130/0091-7613(1984)122.0.CO;2.

Conrad, W.K., 1984, The mineralogy and petrology of compositionally zoned ash flow tuffs, and related silicic rocks, from the McDermitt caldera complex, Nevada-Oregon: Journal of Geophysical Research, v. 89, p. 8639–8664.

Dilles, J.H., and Gans, P.B., 1995, The chronology of Cenozoic volcanism and deformation in the Yerington area, western Basin and Range and Walker Lane: Geological Society of America Bulletin, v. 107, p. 474–486, doi: 10.1130/0016-7606(1995)1072.3.CO;2.

Duffield, W.A., and Dalrymple, G.B., 1990, The Taylor Creek Rhyolite of New Mexico; a rapidly emplaced field of lava domes and flows: Bulletin of Volcanology, v. 52, p. 475–487, doi: 10.1007/BF00268927.

Duffield, W.A., and McKee, E.H., 1986, Geochronology, structure, and basin-range tectonism of the Warner Range, northeastern California: Geological Society of America Bulletin, v. 97, p. 142–146, doi: 10.1130/0016-7606(1986)972.0.CO;2.

Dumitru, T.A., 2000, Fission-track geochronology in Quaternary geology, *in* Noller, J.S., et al., eds., Quaternary geochronology: Methods and applications: American Geophysical Union Reference Shelf, v. 4, p. 131–156.

Egger, A.E., Dumitru, T.A., Miller, E.L., Savage, C.F.I., and Wooden, J.L., 2003, Timing and nature of Tertiary plutonism and extension in the Grouse Creek Mountains, Utah, *in* Ernst, G.W., et al., eds., The Thompson Volume—The lithosphere of western North America and its geophysical characterization: International Geology Review, v. 45, p. 497–532.

Fitzgerald, P.G., Fryxell, J.E., and Wernicke, B.P., 1991, Miocene crustal extension and uplift in southeastern Nevada, constraints from fission-track analysis: Geology, v. 19, p. 1013–1016, doi: 10.1130/0091-7613(1991)0192.3.CO;2.

Foulger, G.R., Anderson, D.L., and Natland, J.H., 2004, Plume IV: Beyond the plume hypothesis—Tests of the plume paradigm and alternatives: GSA Today, v. 14, no. 1, p. 26–28, doi: 10.1130/1052-5173(2004)0142.0.CO;2.

Galbraith, R.F., 1981, On statistical models for mixed fission-track ages: Nuclear Tracks and Radiation Measurements, v. 5, p. 471–478.

Galbraith, R.F., and Laslett, G.M., 1993, Statistical models for mixed fission-track ages: Nuclear Tracks and Radiation Measurements, v. 21, p. 459–470, doi: 10.1016/1359-0189(93)90185-C.

Gans, P.B., Mahood, G.A., and Schermer, E.R., 1989, Synextensional magmatism in the Basin and Range province: A case study from the eastern Great Basin: Geological Society of America Special Paper 233, 53 p.

Gilbert, C.M., and Reynolds, M.W., 1973, Character and chronology of basin development, western margin of the Basin and Range province: Geological Society of America Bulletin, v. 84, p. 2489–2510, doi: 10.1130/0016-7606(1973)842.0.CO;2.

Gleadow, A.J.W., Duddy, I.R., Green, P.F., and Lovering, J.F., 1986, Confined fission track lengths in apatite; a diagnostic tool for thermal history analysis: Contributions to Mineralogy and Petrology, v. 94, p. 405–415.

Graichen, R.E., 1972, Geology of a northern part of the Pine Forest Mountains, Nevada [M.S. thesis]: Corvallis, Oregon State University, 121 p.

Green, P.F., 1981, A new look at statistics in fission-track dating: Nuclear Tracks and Radiation Measurements, v. 5, p. 77–86.

Green, P.F., Duddy, I.R., Laslett, G.M., Hegarty, K.A., Gleadow, A.J.W., and Lovering, J.F., 1989, Thermal annealing of fission tracks in apatite: 4. Quantitative modelling techniques and extension to geological time scales: Chemical Geology, v. 79, p. 155–182.

Hart, W.K., Carlson, R.W., and Mosher, S.A., 1989, Petrogenesis of the Pueblo Mountains basalt, southeastern Oregon and northern Nevada, *in* Reidel, S.P., and Hooper, P.R., eds., Volcanism and Tectonism in the Columbia River flood-basalt province: Geological Society of America Special Paper 239, p. 367–378.

Hooper, P.R., Binger, G.B., and Lees, K.R., 2002, Ages of the Steens and Columbia River flood basalts and their relationship to extension-related calc-alkaline volcanism in eastern Oregon: Geological Society of America Bulletin, v. 114, p. 43–50, doi: 10.1130/0016-7606(2002)1142.0.CO;2.

Howard, K.A., 2003, Crustal structure in the Elko-Carlin region, Nevada, during Eocene gold mineralization: Ruby–East Humboldt metamorphic core complex as a guide to the deep crust: Economic Geology and Bulletin of the Society of Economic Geologists, v. 98, p. 249–268.

Hudson, J.R., John, D.A., Conrad, J.E., and McKee, E.H., 2000, Style and age of late Oligocene–early Miocene deformation in the southern Stillwater Range, west-central Nevada: Paleomagnetism, geochronology, and field relations: Journal of Geophysical Research, v. 105, p. 929–954, doi: 10.1029/1999JB900338.

Humphreys, E.D., 1995, Post-Laramide removal of the Farallon Slab, Western United States: Geology, v. 23, p. 987–990, doi: 10.1130/0091-7613(1995)0232.3.CO;2.

Hurford, A.J., and Green, P.F., 1983, The zeta age calibration in fission-track dating: Chemical Geology, v. 41, p. 285–317.

Jennings, C.W., Strand, R.G., and Rogers, T.H., 1977, Geologic map of California: California Division of Mines and Geology, scale 1:750,000.

Johnson, J.A., Hawkesworth, C.J., Hooper, P.R., and Binger, G.B., 1998, Major and trace element analyses of Steens Basalt, southeastern Oregon: U.S. Geological Survey Open-File Report 98-482, 26 p.

Le Maitre, R.W., Bateman, P., Dudek, A., Keller, J., Lemeyre, J., Le Bas, M.J., Sabine, P.A., Schmid, R., Sorensen, H., Streckeisen, A., Wooley, A.R., and Zanettin, B., 1989, Igneous rocks: A classification and glossary of terms: Oxford, Blackwell, 252 p.

Lerch, D.W., McWilliams, M.O., Miller, E.L., and Colgan, J.P., 2004, Structure and magmatic evolution of the northern Black Rock Range, Nevada: Preparation for a wide-angle refraction/reflection survey: Geological Society of America Abstracts with Programs, v. 36, no. 4, p. 37.

Masuda, A., Nakamura, N., and Tanaka, T., 1973, Fine-structures of mutually normalised rare-earth patterns of chondrites: Geochimica et Cosmochimica Acta, v. 37, p. 239–248, doi: 10.1016/0016-7037(73)90131-2.

Miller, E.L., Dumitru, T.A., Brown, R.W., and Gans, P.B., 1999, Rapid Miocene slip on the Snake Range–Deep Creek Range fault system, east-central Nevada: Geological Society of America Bulletin, v. 111, p. 886–905, doi: 10.1130/0016-7606(1999)1112.3.CO;2.

Minor, S.A., 1986, Stratigraphy and structure of the western Trout Creek and northern Bilk Creek Mountains, Harney County, Oregon, and Humboldt County, Nevada [M.S. thesis]: Boulder, University of Colorado, 177 p.

Noble, D.C., McKee, E.H., Smith, J.G., and Korringa, M.K., 1970, Stratigraphy and geochronology of Miocene volcanic rocks in northwestern Nevada: U.S. Geological Survey Professional Paper 700D, p. 23–32.

Pierce, L.A., and Morgan, K.L., 1992, The track of the Yellowstone hotspot: Volcanism, faulting, and uplift, *in* Link, P.K., et al., eds., Regional geology of eastern Idaho and western Wyoming: Geological Society of America Memoir 179, p. 1–53.

Renne, P.R., Swisher, C.C., Deino, A.L., Karner, D.B., Owens, T.L., and DePaolo, D.J., 1998, Intercalibration of standards, absolute ages and uncertainties in $^{40}Ar/^{39}Ar$ dating: Chemical Geology, v. 145, p. 117–152, doi: 10.1016/S0009-2541(97)00159-9.

Roback, R.C., van der Meulen, D.B., King, H.D., Plouff, D., Munts, S.R., and Willet, S.L., 1987, Mineral resources of the Pueblo Mountains Wilderness study area, Harney County, Oregon, and Humboldt County, Nevada: U.S. Geological Survey Bulletin 1740-B, p. B1–B30, map scale 1:48,000.

Rytuba, J.J., and McKee, E.H., 1984, Peralkaline ash flow tuffs and calderas of the McDermitt volcanic field, southeast Oregon and north central Nevada: Journal of Geophysical Research, v. 89, p. 8616–8628.

Saltus, R.W., and Jachens, R.C., 1995, Gravity and basin-depth maps of the Basin and Range province, western United States: U.S. Geological Survey Geophysical Investigations Map GP-1012, scale 1:2,500,000, 1 sheet.

Smith, D.L., 1992, History and kinematics of Cenozoic extension in the northern Toiyabe Range, Lander County, Nevada: Geological Society of America Bulletin, v. 104, p. 789–801, doi: 10.1130/0016-7606(1992)1042.3.CO;2.

Smith, D.L., Gans, P.B., Miller, E.L., Lisle, R.E., Schafer, R.W., and Wilkinson, W.H., 1991, Palinspastic restoration of Cenozoic extension in the central and eastern Basin and Range Province at latitude 39–40 degrees N, *in* Raines, G.L., et al., eds., Geology and ore deposits of the Great Basin: Reno, Nevada, Geological Society of Nevada, p. 75–86.

Smith, J.G., 1973, Geologic map of the Duffer Peak Quadrangle, Humboldt County, Nevada: U.S. Geological Survey Geologic Investigations Map I-606, scale 1:48,000.

Steiger, R.H., and Jäger, E., 1977, Subcommission on geochronology: Convention on the use of decay constants in geo- and cosmochronology: Earth and Planetary Science Letters, v. 36, p. 359–362, doi: 10.1016/0012-821X(77)90060-7.

Stewart, J.H., 1980, The geology of Nevada: Nevada Bureau of Mines and Geology Special Publication 4, 136 p.

Stewart, J.H., and Carlson, J.E., 1978, Geologic map of Nevada: U.S. Geological Survey, scale 1:500,000.

Stockli, D.F., 1999, Regional timing and spatial distribution of Miocene extension in the northern Basin and Range Province [Ph.D. thesis]: Stanford, California, Stanford University, 239 p.

Stockli, D.F., Linn, J.K., Walker, J.D., and Dumitru, T.A., 2001, Miocene unroofing of the Canyon Range during extension along the Sevier Desert Detachment, west-central Utah: Tectonics, v. 20, p. 289–307, doi: 10.1029/2000TC001237.

Stockli, D.F., Dumitru, T.A., McWilliams, M.O., and Farley, K.A., 2003, Cenozoic tectonic evolution of the White Mountains: California and Nevada: Geological Society of America Bulletin, v. 115, p. 788–816, doi: 10.1130/0016-7606(2003)1152.0.CO;2.

Surpless, B.E., Stockli, D.F., Dumitru, T.A., and Miller, E.L., 2002, Two-phase westward encroachment of Basin and Range extension into the northern Sierra Nevada: Tectonics, v. 21, p. 2-1–2-13, doi: 10.1029/2000TC001257.

Swisher, C.C., 1992, $^{40}Ar/^{39}Ar$ dating and its application to the calibration of the North American land mammal ages [Ph.D. thesis]: Berkeley, University of California, 239 p.

Walker, G.W., and MacLeod, N.S., 1991, Geologic map of Oregon: U.S. Geological Survey Special Geologic Map, 2 sheets, scale 1:500,000.

Wernicke, B.P., 1992, Cenozoic extensional tectonics, *in* Burchfiel, B.C., et al., eds., The Cordilleran orogen: Conterminous U.S.: Boulder, Colorado, Geological Society of America, Geology of North America, v. G-3, p. 553–581.

Wyld, S.J., 1996, Early Jurassic deformation in the Pine Forest Range, northwest Nevada, and implications for Cordilleran tectonics: Tectonics, v. 15, p. 566–583, doi: 10.1029/95TC03693.

Wyld, S.J., 2002, Structural evolution of a Mesozoic back-arc fold-and-thrust belt in the U.S. Cordillera: New evidence from northwestern Nevada: Geological Society of America Bulletin, v. 114, p. 1452–1486, doi: 10.1130/0016-7606(2002)1142.0.CO;2.

Wyld, S.J., and Wright, J.E., 2001, New evidence for Cretaceous strike-slip faulting in the United States Cordillera, and implications for terrane-displacement, deformation patterns, and plutonism: American Journal of Science, v. 301, p. 150–181.

Manuscript Received by the Society 19 July 2004
Revised Manuscript Received 9 April 2005
Manuscript Accepted 4 May 2005

Printed in the USA